

Co-Design of Delays and Sparse Controllers for Bandwidth-Constrained Cyber-Physical Systems

Nandini Negi^{1,2} and Aranya Chakraborty^{1,3}

¹Electrical & Computer Engineering, North Carolina State University

Email : ²nnegi@ncsu.edu, ³aranya.chakraborty@ncsu.edu *

Abstract

We address the problem of sparsity-promoting optimal control of cyber-physical systems with feedback delays. The delays are categorized into two classes - namely, intra-layer delay, and inter-layer delay between the cyber and the physical layers. Our objective is to minimize the \mathcal{H}_2 -norm of the closed-loop system by designing an optimal combination of these two delays along with a sparse state-feedback controller, while respecting a given bandwidth constraint. We propose a two-loop optimization algorithm for this. The inner loop, based on alternating directions method of multipliers (ADMM), handles the conflicting directions of decreasing \mathcal{H}_2 -norm and increasing sparsity of the controller. The outer loop comprises of semidefinite program (SDP)-based relaxations of non-convex inequalities necessary for stable co-design of the delays with the controller. We illustrate this algorithm using simulations that highlight various aspects of how delays and sparsity impact the stability and \mathcal{H}_2 -performance of a LTI system.

1 Introduction

In recent years, sparsity-promoting optimal control has emerged as a key tool for enabling economical control of large-scale cyber-physical systems (CPSs). such as ADMM [1], LASSO [2], GraSP [3], and PALM [4]. An extension of these results to LTI systems with communication delays has been reported in [5]. Since most real-world CPSs operate under stringent constraints for bandwidth, stability and closed-loop performance in the presence of delays are important requirements for these controllers [6]. Accordingly, the algorithm in [5] derives convex relaxations of bilinear matrix inequalities to design a sparse controller, while guaranteeing closed-loop stability under a constant delay.

In this paper, we extend the design in [5] one step further by considering the delays themselves as *design variables*. Our formulation is motivated by modern CPS communication technologies such as software-defined networking (SDN) and cloud computing that offer flexibility to network operators in choosing delays in communication links. We consider two kinds of delays - namely (1) *inter-layer* delay that arises in the local-area network (LAN) connecting the sensors in the physical layer to the computational units in the cyber layer, and (2) *intra-layer* delay that arises in the SDN connecting the computational units spread across the cyber-layer. Our goal is to co-design these two delays with a sparse feedback controller so that the \mathcal{H}_2 -norm of the closed-loop system is minimized, while ensuring that both delays are greater than or equal to their individual lower bounds that arise from the cost of the network bandwidth. The main contribution of this paper is to develop a hierarchical optimization algorithm that provides a guided solution for this co-design. The outer loop designs

*The research presented in this paper was partly supported by the US National Science Foundation under grant ECCS 1509137.

the two delays and finds a corresponding stabilizing controller by sequentially relaxing the non-linear matrix equations required for the co-design. The inner loop sparsifies this controller while minimizing the closed-loop \mathcal{H}_2 -norm. Our results show that depending on the plant dynamics, the relative magnitudes of the two delays for achieving the optimal \mathcal{H}_2 -norm can be notably different.

Note that our problem is fundamentally different from the conventional bandwidth allocation and delay assignment problems commonly addressed in the networking literature [7], [8], where the utility functions to be optimized are static objectives. Our goal, in contrast, is to design a bandwidth allocation mechanism that minimizes the \mathcal{H}_2 -norm of a CPS over a sparse state-feedback controller. We illustrate the effectiveness of our algorithm using simulations that highlight the impacts of delays and sparsity on \mathcal{H}_2 -performance.

The rest of the paper is organized as follows. Section 2 states the problem formulation followed by Section 3 that describes the proposed co-design of the delays. Section 4 introduces the two-loop algorithm to solve the problem followed by simulations in Section 5, and conclusion in Section VI. The proofs of all lemmas, theorems and propositions are listed in the Appendix unless stated otherwise.

2 Problem Formulation

2.1 State Feedback with Communication Delays

Consider a LTI system with the following dynamics:

$$\dot{x}(t) = Ax(t) + Bu(t) + B_w w(t), \quad (1)$$

where $x \in \mathbb{R}^n$ is the state, $u \in \mathbb{R}^m$ is the control, and $w \in \mathbb{R}^r$ is the exogenous input, with the corresponding matrices $A \in \mathbb{R}^{n \times n}$, $B \in \mathbb{R}^{n \times m}$ and $B_w \in \mathbb{R}^{n \times r}$. We design a state-feedback controller, ideally represented as $u(t) = -Kx(t)$. However, due to limited bandwidth availability, the controller includes finite delays in the feedback. The CPS model that we consider is described as follows.

1. There are p sensors and actuators in the physical layer and the state vector $x(t)$ is correspondingly divided into p non-overlapping parts $\bar{x}_1(t), \dots, \bar{x}_p(t)$, where \bar{x}_i is measured by the i -th sensor.
2. There are p computing units or control nodes located in a virtual cloud network. The i -th sub-state $\bar{x}_i(t)$ is transmitted to the i -th control node through LAN with incident delay $\tau_d/2$.
3. Inside the cloud, also referred to as the *cyber layer*, the control nodes share their individual sub-states $\bar{x}_i(t)$ with each other over an SDN with delay τ_c . Each control node i calculates a portion of the control input vector denoted as $\bar{u}_i(t) \in \mathbb{R}^{m_i}$, where $\sum_{i=1}^p m_i = m$.
4. The calculated control inputs are transmitted back to the physical layer with $\tau_d/2$ delay.

A schematic of this CPS with $n = 3$, $m = 2$ and $p = 2$ is shown in Fig. 1. Denoting $\tau_o = \tau_d + \tau_c$, the control input can be expressed as:

$$u(t) = -\underbrace{(K \circ \mathcal{I}_d)}_{K_d} x(t - \tau_d) - \underbrace{(K \circ \mathcal{I}_o)}_{K_o} x(t - \tau_o), \quad (2)$$

where \circ represents Hadamard product. $\mathcal{I}_d, \mathcal{I}_o \in \mathbb{R}^{m \times n}$ are binary matrices such that

$$\mathcal{I}_d(i, j) = \begin{cases} 1, & \text{If } \exists q \in \{1, \dots, p\} : u_i \in \bar{u}_q \text{ and } x_j \in \bar{x}_q, \\ 0, & \text{otherwise.} \end{cases} \quad (3)$$

and \mathcal{I}_o is the complement of \mathcal{I}_d . For the system shown in Fig. 1, \mathcal{I}_d and \mathcal{I}_o are:

$$\mathcal{I}_d = \begin{matrix} & \overbrace{\begin{matrix} \bar{x}_1 & \bar{x}_2 \end{matrix}} & \\ \begin{matrix} \bar{u}_1 \\ \bar{u}_2 \end{matrix} & \begin{bmatrix} 1 & 1 & 0 \\ 0 & 0 & 1 \end{bmatrix} \end{matrix}, \quad \mathcal{I}_o = \begin{matrix} & \overbrace{\begin{matrix} \bar{x}_1 & \bar{x}_2 \end{matrix}} & \\ \begin{matrix} \bar{u}_1 \\ \bar{u}_2 \end{matrix} & \begin{bmatrix} 0 & 0 & 1 \\ 1 & 1 & 0 \end{bmatrix} \end{matrix}. \quad (4)$$

The closed-loop system of (1)-(2) can be written as:

$$\begin{aligned} \dot{x}(t) &= Ax(t) - BK_d x(t - \tau_d) - BK_o x(t - \tau_o) + B_w w(t), \\ z(t) &= Cx(t) + Du(t) = \begin{bmatrix} Q^{1/2} \\ 0 \end{bmatrix}, \quad D = \begin{bmatrix} 0 \\ R^{1/2} \end{bmatrix}, \end{aligned} \quad (5)$$

where $z(t)$ is the measurable output, $Q \geq 0$ and $R > 0$. We make the standard assumption that (A, B) and $(A, Q^{1/2})$ are stabilizable and detectable, respectively [1, Sec. II].

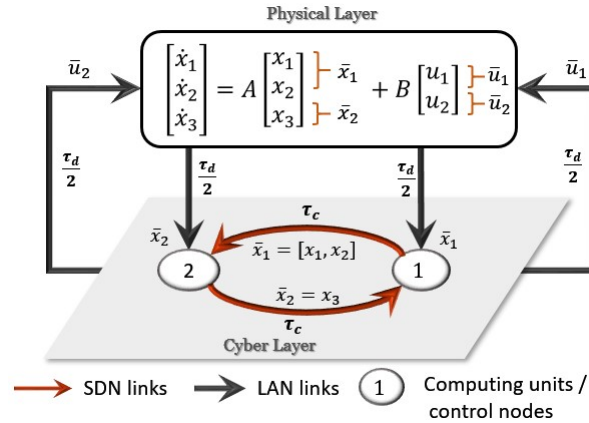


Figure 1: Sample CPS schematic showing physical and cyber layers with the associated delays.

2.2 Problem Setup

Our goal is to design a K that minimizes the \mathcal{H}_2 -norm of the transfer function from $w(t)$ to $z(t)$ for the time-delayed LTI system (5). In general, the \mathcal{H}_2 -performance of (5) will be worse than that of the delay-free system [9, Section 5.6.1]. Therefore, reducing both the delays τ_d and τ_c will improve the \mathcal{H}_2 -performance. The trivial solution, of course, would be to use $\tau_d = \tau_o = 0$, which is not possible in reality as that would require infinite bandwidth.

Let the combined bandwidth of links connecting the physical sensors to the cloud be W_{cp} , and that of SDN links inside the cloud be W_{cc} . Then, the total cost for renting bandwidth can be written as:

$$S = m_{cp}W_{cp} + m_{cc}W_{cc}, \quad (6)$$

where m_{cp} and m_{cc} are the respective dollar costs for renting LAN and SDN links. W_{cp} and W_{cc} are divided into the total number of links as described below.

- The uplink for carrying $\bar{u}_i(t)$ back to the physical actuator is not needed if the i -th block row of K is entirely 0. Similarly, if the i -th block column of K is 0, then \bar{x}_i is no longer required for calculating any control input, and the corresponding downlink becomes redundant. The uplinks and downlinks together constitute the LAN links. Thus, W_{cp} is effectively divided into the number of non-zero block rows and columns of K denoted by $N_{row}(K)$ and $N_{col}(K)$, respectively.
- W_{cc} is divided into the number of non-zero off-diagonal blocks of K denoted by $N_{off}(K)$.

Accordingly, we can write the bandwidth constraint as:

$$S = 2m_{cp} \left(\frac{N_{row}(K) + N_{col}(K)}{\tau_d} \right) + m_{cc} \left(\frac{N_{off}(K)}{\tau_o - \tau_d} \right) \leq S_b, \quad (7)$$

where $S_b > 0$ is a mandatory budget that is imposed to prevent infinite bandwidth. To minimize the cost of renting the links and bandwidth, we wish to reduce the number of both LAN and SDN links by promoting sparsity in K . Our design objectives, therefore, are listed as:

P1 : Design τ_d , τ_o and K such that

- \mathcal{H}_2 -norm of the closed-loop transfer function of (5) from $w(t)$ to $z(t)$, denoted as J , is minimized.
- The bandwidth cost S satisfies (7) for some given budget S_b , which is assumed to be large enough for the problem to be feasible.
- Sparsity of K is promoted.

Let \mathbb{K} be the set of all K that stabilize (5) for given delays τ_o and τ_d . Given S_b , **P1** can be mathematically stated as:

$$\underset{K, \tau_d, \tau_o}{\text{minimize}} \quad J(K, \tau_d, \tau_o) + g(K), \quad (8a)$$

$$\text{subject to} \quad K \in \mathbb{K}, \quad (8b)$$

$$S(\tau_d, \tau_o, K) \leq S_b, \quad (8c)$$

where S is given by (7), and $g(K)$ is a sparsity-promoting function which will be introduced in Section 4.1. The closed-form expression of J is derived next.

2.3 \mathcal{H}_2 norm for the Delayed System

The delayed system (5) is infinite dimensional. In order to obtain a linear, finite dimensional LTI approximation of (5), we use the method of spectral discretization given in [10]. Since $\tau_o > \tau_d$ in (5), following [10], we divide $[-\tau_o, 0]$ into a grid of N scaled and shifted Chebyshev extremal points

$$\theta_{k+1} = \frac{\tau_o}{2} \left(\cos \left(\frac{(N-k-1)\pi}{N-1} \right) - 1 \right), \quad k = \{0, \dots, N-1\}, \quad (9)$$

such that $\theta_1 = -\tau_o$ and $\theta_N = 0$. The choice of N is guided by [10, Section 4]. Let $v(\theta) = x(t + \theta)$ denote the θ -shifted state vector. The extended state η and the closed-loop state matrix A_{cl} can then be written as:

$$\eta = [v^T(\theta_1), \dots, v^T(\theta_N) = x(t)]^T, \quad l_j(\theta) = \prod_{m=1, m \neq j}^N \frac{\theta - \theta_m}{\theta_j - \theta_m}, \quad (10a)$$

$$A_{clij} = \begin{cases} \partial_\theta l_j(\theta_i) I_n, & j = 1, \dots, N, i = 1, \dots, N-1 \\ l_N(-\tau_d) B K_d + A, & j = N, i = N \\ l_1(-\tau_d) B K_d + B K_o, & j = 1, i = N \\ l_j(-\tau_d) B K_d, & j = 2, \dots, N-1, i = N, \end{cases} \quad (10b)$$

where $K_d = K \circ \mathcal{I}_d$, $K_o = K \circ \mathcal{I}_o$. We can separate A_{cl} into three sub-components:

$$A_{cl} = \tilde{A} - \mathcal{B} K_o N_o^T - \mathcal{B} K_d N_d^T, \quad (11)$$

$$\mathcal{B} = MB, \quad M = [\mathbf{0}, \dots, \mathbf{0}, I_n]^T, \quad N_o = [I_n, \mathbf{0}, \dots, \mathbf{0}]^T, \quad (12)$$

where the first sub-component \tilde{A} is independent of K_d and K_o , the second is only dependent on K_o , and the third on K_d . The explicit expressions for \tilde{A} and N_d in terms of τ_d and τ_o will be derived shortly in the next section. The linear approximation of the closed-loop system (5) becomes:

$$\dot{\eta}(t) = A_{cl}\eta(t) + \mathcal{B}_w w(t), \quad (13a)$$

$$z(t) = \mathcal{C}\eta(t), \quad \mathcal{C} = \begin{bmatrix} Q^{1/2} M^T \\ -R^{1/2} (K_d N_d^T + K_o N_o^T) \end{bmatrix}, \quad (13b)$$

where $\mathcal{B}_w = MB_w$. The algebraic Riccati equations (AREs) and the closed-loop \mathcal{H}_2 -norm J can be written as:

$$A_{cl}^T P + P A_{cl} = -\mathcal{C}^T \mathcal{C} = -(\tilde{Q} + \tilde{C}^T R \tilde{C}), \quad (14)$$

$$A_{cl} L + L A_{cl}^T = -\mathcal{B} \mathcal{B}^T, \quad (15)$$

$$J(K, \tau_d, \tau_o) = \text{Tr}(\mathcal{B}^T P \mathcal{B}) = \text{Tr}(\mathcal{C} L \mathcal{C}^T). \quad (16)$$

where $\tilde{Q} = M Q M^T$ and $\tilde{C} = (K_d N_d^T + K_o N_o^T)$.

3 Derivation of the gradient of \mathcal{H}_2 norm

Our goal is to design (K, τ_d, τ_o) to minimize J . However, from (14)-(16), we see that J is a function of \tilde{A} and N_d , besides K . To compute the gradient of J with respect to (K, τ_d, τ_o) , it is important to express \tilde{A} and N_d in terms of these three design variables. We begin this section with these derivations as follows.

3.1 \mathcal{H}_2 Performance and Design Variables

Recall that the closed-loop state matrix $A_{cl} = \tilde{A} - \mathcal{B}(K_o N_o^T + K_d N_d^T)$. In the next two lemmas, we express A_{cl} as a function of τ_o , K and the delay ratio $c = \tau_d/\tau_o$.

Lemma 1 \tilde{A} is a function of τ_o , and can be written as:

$$\tilde{A} = \frac{1}{\tau_o} \Lambda + \bar{A}, \quad \bar{A} = \text{Diag}(\mathbf{0}, A), \quad (17)$$

where Λ is a constant matrix for constant N . ■

Lemma 2 N_d is a function of the ratio $c = \tau_d/\tau_o \in [0, 1]$, and can be written as:

$$N_d(c) = (\Gamma \nu(c)) \otimes I_n, \quad \nu(c) = [c^{N-1} \ c^{N-2} \ \dots \ c^2 \ c \ 1]^T, \quad (18)$$

where $\Gamma \in \mathbb{R}^{N \times N}$ is a constant matrix for constant N . ■

Lemmas 1 and 2 show that for fixed N , J for the system in (13) can be written as a function of τ_o and c . Henceforth, all of our analysis for minimizing J will be carried out using τ_o and c , instead of τ_o and τ_d . This change of variables is invertible, and therefore, there is no loss of generality.

3.2 Gradient of \mathcal{H}_2 norm

In order to minimize J , we next derive the gradient of J . We define a set \mathcal{K} as:

$$\mathcal{K} := \{(K, \tau_o, c) : \text{Re}(\lambda(A_{cl})) < 0\}, \quad (19)$$

i.e., the set of solutions that guarantee closed-loop stability of (13). Given this definition, we first prove the existence of a unique solution of (14) and differentiability of P , followed by the derivation of ∇J . For the rest of the paper, the $A'(B)$ notation represents differentiability of A depending on B .

Lemma 3 *Let $(K, \tau_o, c) \in \mathcal{K}$. Then, there exists a unique solution $P(K, \tau_o, c)$ of (14). Moreover, P is differentiable with respect to the variables τ_o , c and K on \mathcal{K} . Specifically, $P'(\tau_o)d\tau_o$, $P'(c)dc$ and $P'(K)dK$ follow as solutions of the following Lyapunov equations, respectively:*

$$A_{cl}^T P'(\tau_o) d\tau_o + P'(\tau_o) d\tau_o A_{cl} = \frac{d\tau_o}{\tau_o^2} (\Lambda^T P + P \Lambda), \quad (20)$$

$$A_{cl}^T P'(c) dc + P'(c) dc A_{cl} = N'_d dc K_d^T G + G^T K_d N_d^T dc, \quad (21)$$

$$A_{cl}^T P'(K) dK + P'(K) dK A_{cl} = -Z_d - Z_d^T - Z_o - Z_o^T, \quad (22)$$

where $G = (R(K_d N_d^T(c) + K_o N_o^T) - \mathcal{B}^T P)$, $Z_d = N_d^T (dK \circ \mathcal{I}_d) G$, $Z_o = N_o^T (dK \circ \mathcal{I}_o) G$ and $N'_d = (\Gamma \partial \nu(c)) \otimes I_n$. ■

We next use Lemma 3 to state the following theorem.

Theorem 1 *J in (16) is differentiable on \mathcal{K} . The gradient of J is evaluated as:*

$$J'(\tau_o) = -\frac{2}{\tau_o^2} \text{Tr}(\Lambda^T P L), \quad J'(c) = 2 \text{Tr}(N'_d K_d^T G L), \quad (23)$$

$$\nabla J(K) = 2((GLN_d) \circ \mathcal{I}_d + (GLN_o) \circ \mathcal{I}_o). \quad (24)$$

The negative directions of $J'(c)$ and $J'(\tau_o)$, as derived in Theorem 1, always point to the trivial solution $c = 0$, $\tau_o = 0$ which defeats the purpose of designing τ_d and τ_o . This is because the partial derivatives in (23)-(24) are derived with the assumption that K , τ_o and c are independent of each other as $K'(\tau_o)$ and $K'(c)$ cannot be computed directly given the implicit dependence of K on τ_o and c . Therefore, it would be incorrect to co-design c , τ_o and K using just the gradient information. Starting from a stabilizing $(K, \tau_o, c) \in \mathcal{K}$, as soon as we change either τ_o or c , we must update K to ensure stability of (13). In other words, (K, τ_o) and (K, c) must be co-designed separately in sequence while holding c and τ_o as constant in the respective steps.

3.3 Co-design of Controller and Delays

We next describe how equations in (14)-(15) can be relaxed for each of the two co-designs.

- **Co-design of (K, τ_o)**

Theorem 2 Let $\omega_o = 1/\tau_o$. Consider a known tuple $(K^*, \omega_o^*, c^*) \in \mathcal{K}$ satisfying (14) with a known P^* for closed-loop state matrix $A_{cl}^*(K^*, \omega_o^*, c^*)$. Let $\omega_o = \omega_o^* + \Delta\omega$, $K = K^* + \Delta K$, $P = P^* + \Delta P$ and $\alpha \in \mathbb{R}$ be obtained as a solution of the following SDP:

$$\phi_0 + \phi_1 + \psi_0 + \alpha I \geq 0, \quad (25a)$$

$$|\Delta\omega| \leq \zeta_1, \quad \|\Delta P\| \leq \zeta_2, \quad (25b)$$

$$\alpha \geq 2\zeta_1 \|\Lambda^T \Delta P\| + 2\zeta_2 \|\mathcal{B} \Delta \tilde{C}\| + \|R^{1/2} \Delta \tilde{C}\|^2, \quad (25c)$$

where α , ΔK , ΔP and $\Delta\omega$ are the design variables. Then, $(K, 1/\omega_o, c^*)$ is a stabilizing tuple for (13). In (25), $\phi_0 = A_{cl}^{*T} P + P A_{cl}^*$, $K_d^* = K^* \circ \mathcal{I}_d$, $\Delta K_d = \Delta K \circ \mathcal{I}_d$, $K_o^* = K^* \circ \mathcal{I}_o$, $\Delta K_o = \Delta K \circ \mathcal{I}_o$, $\tilde{C}^* = \tilde{Q} + (K_d^* N_d^T + K_o^* N_o^T)$, $\Delta \tilde{C} = (\Delta K_d N_d^T + \Delta K_o N_o^T)$, $A_1 = -\mathcal{B}(\Delta \tilde{C}) + \Delta\omega \Lambda$, $\phi_1 = A_1^T P^* + P^* A_1$, $\psi_0 = \tilde{C}^{*T} R \tilde{C}^* + \Delta \tilde{C}^T R \tilde{C} + \tilde{C}^* R \Delta \tilde{C}$ and, ζ_1, ζ_2 are chosen constants. ■

• **Co-design of (K, c)**

Next, consider the co-design step for (K, c) . Recall that A_{cl} is a non-linear function of $c \in [0, 1]$ through $N_d(c)$ as shown in Lemma 2, and therefore, the exact expression of $N_d(c)$ cannot be used while forming the SDP relaxations. To circumvent this problem, we divide $[0, 1]$ into k_c sub-intervals $[c_1, c_2], [c_2, c_3], \dots, [c_{k_c}, c_{k_c+1}]$ with each sub-interval small enough to allow $N_d(c)$ to be approximated as an affine function $\hat{N}_d(c)$. Let each sub-interval $[c_i, c_{i+1}]$ have an associated $\chi^{(i)} \in \mathbb{R}^{N \times 2}$ as the vector of affine coefficients. The approximated function is written as:

$$\hat{N}_d(c) = \left(\chi^{(i)} [c, 1]^T \right) \otimes I_n, \quad c \in [c_i, c_{i+1}], \quad i = 1, \dots, k_c. \quad (26)$$

The coefficients can be computed from a linear curve fitting on (18). Larger the number of sub-intervals k_c , lower is the approximation error $\|\hat{N}_d - N_d\|$. For our simulations in Section 5, we have used $k_c = 10$. We next present the SDP relaxation for the co-design of (K, c) .

Theorem 3 Consider a known tuple $(K^*, \tau_o^*, c^*) \in \mathcal{K}$ with $c^* \in [c_i, c_{i+1}]$ for some $i \in \{1, \dots, k_c\}$ satisfying (15) with a known L^* for closed-loop state matrix $A_{cl}^*(K^*, \tau_o^*, c^*)$. Let $c = c^* + \Delta c$, $K = K^* + \Delta K$, $L = L^* + \Delta L$ and $\alpha \in \mathbb{R}$ be a solution of the following SDP:

$$\phi_0 + \phi_1 + \mathcal{B} \mathcal{B}^T + \alpha I \geq 0, \quad (27a)$$

$$c_i \leq c \leq c_{i+1}, \quad \|\Delta L\| \leq \beta, \quad (27b)$$

$$\begin{aligned} \alpha \geq & 2\beta \|\mathcal{B}(\Delta K_d N_d^T(c^*) + \Delta K_o N_o^T)\| + 2\beta \mathfrak{S} \|\mathcal{B} \Delta K_d\| \\ & + 2\beta \|\Delta N_d K_d^{*T} B^T M^T\| + 2\mathfrak{S} \|\mathcal{B} \Delta K_d\| \|L^*\|, \end{aligned} \quad (27c)$$

where α , ΔK , ΔP and Δc are the design variables. Then, (K, τ_o^*, c) is a stabilizing tuple for (13). In (27), $\Delta N_d = \hat{N}_d(c) - N_d(c^*)$, $\phi_0 = A_{cl}^* L + L A_{cl}^{*T}$, $\phi_1 = A_1 L^* + L^* A_1^T$, $A_1 = -\mathcal{B}(K_d^* \Delta N_d^T(c) + \Delta K_d N_d^T(c^*) + \Delta K_o N_o^T)$. The scalar β is a chosen constant, and $\mathfrak{S} \geq \|N_d(c)\|$. ■

Starting from a known stabilizing tuple (K^*, τ_o^*, c^*) , Theorems 2 and 3 enable us to co-design new stabilizing pairs (K, τ_o) and (K, c) , respectively. Next, we integrate the bandwidth cost constraint (7) with the SDPs in (25) and (27).

3.4 Incorporating Bandwidth Constraints

We impose the bandwidth cost constraint (7) as part of **P1**, which can be rewritten as:

$$S = 2m_{cp} \left(\frac{N_{row}(K) + N_{col}(K)}{c\tau_o} \right) + m_{cc} \left(\frac{N_{off}(K)}{\tau_o - c\tau_o} \right) \leq S_b. \quad (28)$$

Recall that S is the total bandwidth cost and S_b is the upper bound imposed on it. When (28) is imposed on SDPs (25) and (27), we obtain an alternative form of (28), which is stated in the next proposition.

Proposition 1 Consider a known tuple $(K^*, \tau_o^*, c^*) \in \mathcal{K}$ with an associated bandwidth cost $S^* \leq S_b$. Denoting $n_{cp}^* = N_{row}(K^*) + N_{col}(K^*)$ and $n_{cc}^* = N_{off}(K^*)$, the following statements are true.
1) Keeping $\tau_o = \tau_o^*$, let c^* be perturbed to c resulting in a cost S . Then, $\delta S(c) := S - S^*$ is a convex function of c :

$$\delta S(c) = \frac{(S^* \tau_o^*)c^2 + (m_{cc}n_{cc}^* - 2m_{cp}n_{cp}^* - S^* \tau_o^*)c + 2m_{cp}n_{cp}^*}{c(1-c)\tau_o^*}. \quad (29)$$

The constraint $\delta S(c) \leq 0$ implies $S \leq S_b$.

2) Keeping $c = c^*$, let τ_o^* be perturbed to τ_o , resulting in a new bandwidth cost S . Then, $\delta S(\tau_o) := S - S^*$ is an affine function of τ_o :

$$\delta S(\tau_o) = \frac{1}{S^*} \left(\frac{2m_{cp}n_{cp}^*}{c^*} + \frac{m_{cc}n_{cc}^*}{(1-c^*)} \right) - \tau_o. \quad (30)$$

The constraint $\delta S(\tau_o) \leq 0$ implies $S \leq S_b$.

Proof: The proof follows from simple algebra. ■

Since $\delta S(\tau_o)$ and $\delta S(c)$ are each convex in their respective arguments in the above proposition, we can easily incorporate them in the co-design SDPs of Theorems 2 and 3 to satisfy the bandwidth constraint in (28). Note that since K is co-designed with either τ_o or c , the true bandwidth cost S depends on K as well through $(N_{row}(K) + N_{col}(K))$ and $N_{off}(K)$. If $N_{row}(K) \leq N_{row}(K^*)$, $N_{col}(K) \leq N_{col}(K^*)$ and $N_{off}(K) \leq N_{off}(K^*)$, one can easily verify that $\delta S(c) \leq 0$ and $\delta S(\tau_o) \leq 0$ in (29)-(30) hold, and the true bandwidth costs always satisfy (28). We ensure this fact by imposing a two-loop structure in our design algorithm, as will be seen shortly in the next section. We next bring together the co-design SDPs (25), (27) and bandwidth constraints (29), (30) in the form of our main algorithm.

4 Problem Setup in Two-Loop ADMM Form

The \mathcal{H}_2 -norm J , in general, increases with increasing sparsity of K [5], while the bandwidth cost S reduces. Due to these inherent trade-offs between the objectives and the constraints, **P1** is a prime candidate to be reformulated as a two-loop ADMM optimization. The outer-loop co-designs (K, τ_o) and (K, c) using (25)-(27) under the bandwidth constraints (29)-(30). The inner-loop, on the other hand, sparsifies K while minimizing J . We describe the inner and outer loops in Sections 4.1 and 4.2 respectively, followed by the main algorithm in Section 4.3.

4.1 Inner ADMM Loop

Throughout the inner ADMM loop, we hold both τ_o and c as constants. The mathematical program of the inner loop denoted as **P1_{in}** is written as follows:

$$\mathbf{P1}_{in} : \underset{K, F}{\text{minimize}} \quad J(K) + \lambda g(F), \quad (31a)$$

$$\text{subject to} \quad K = F, \quad (31b)$$

where λ is a regularization parameter and $g(F) = \|W \circ F\|_{l_1}$ is the weighted l_1 norm function which is used to induce sparsity in F . The weight matrix W for $g(F)$ is updated iteratively through a series of reweighting steps from the solution of the previous iteration as [11]:

$$W_{ij} = \frac{1}{|F_{ij}| + \epsilon}, \quad 0 < \epsilon \ll 1. \quad (32)$$

The augmented Lagrangian for $\mathbf{P1}_{\text{in}}$ is

$$\mathcal{L}_p = J(K) + \lambda g(F) + \text{Tr}(\Theta^T(K - F)) + \frac{\rho}{2} \|K - F\|_{\mathbb{F}}^2, \quad (33)$$

where ρ is a positive scalar and Θ is the dual variable. ADMM involves solving each objective separately while simultaneously projecting onto the solution set of the other. As shown in [1, 12], (33) is used to derive a sequence of iterative steps K -min, F -min and Θ -min by completing the squares with respect to each variable.

$$K_{k+1} = \underset{K}{\text{argmin}} \Phi_1(K) = \underset{K}{\text{argmin}} J(K) + \frac{\rho}{2} \|K - U_k\|_{\mathbb{F}}^2, \quad (34a)$$

$$F_{k+1} = \underset{F}{\text{argmin}} \Phi_2(F) = \underset{F}{\text{argmin}} \lambda g(F) + \frac{\rho}{2} \|F - V_k\|_{\mathbb{F}}^2, \quad (34b)$$

$$\Theta_{k+1} = \Theta_k + \rho(K_{k+1} - F_{k+1}), \quad (34c)$$

where $U_k = F_k - \frac{1}{\rho}\Theta_k$ and $V_k = K_{k+1} + \frac{1}{\rho}\Theta_k$. We next present a method to solve K -min and provide an analytical expression for F -min.

4.1.1 K -min Step

Setting $\nabla\Phi_1(K) = 0$ and using Theorem 1, we get the following condition for optimality¹:

$$[(GLN_d) \circ \mathcal{I}_d + (GLN_o) \circ \mathcal{I}_o] + \frac{\rho}{2}(K - U) = 0, \quad (35)$$

where $G = R(K_d N_d^T + K_o N_o^T) - \mathcal{B}^T P$ and $U = U_k$ for the $(k+1)$ -th iteration of the ADMM loop. P and L are the solutions of AREs (14) and (15), respectively. K -min begins with a stabilizing K , solves (14) and (15) for P and L , and then solves (35) to obtain a new gain \bar{K} as follows:

$$\bar{K} = \text{Reshape} \left((\hat{V}_d \circ T_d + \hat{V}_o \circ T_o + \rho I_{n^2})^{-1} \mu, [\mathbf{m}, \mathbf{n}] \right), \quad (36)$$

$$T_d = (T_{dd} \circ \hat{V}_d^T + T_{od} \circ \hat{V}_o^T), \quad T_o = (T_{oo} \circ \hat{V}_o^T + T_{do} \circ \hat{V}_d^T),$$

$$T_{dd} = 2(N_d^T L N_d \otimes R), \quad T_{od} = 2(N_o^T L N_d \otimes R),$$

$$T_{oo} = 2(N_o^T L N_o \otimes R), \quad T_{do} = 2(N_d^T L N_o \otimes R),$$

$$\mu = \text{vec} \left((2\mathcal{B}^T P L N_d) \circ \mathcal{I}_d + (2\mathcal{B}^T P L N_o) \circ \mathcal{I}_o + \rho U \right),$$

$$\hat{V}_d = \mathbf{1} \otimes v_d, \quad v_d = \text{vec}(\mathcal{I}_d), \quad \hat{V}_o = \mathbf{1} \otimes v_o, \quad v_o = \text{vec}(\mathcal{I}_o),$$

The notation $B = \text{Reshape}(A, [p, q])$ is used for an operator that reshapes $A \in \mathbb{R}^{m \times n}$ in row-traversing order to another matrix $B \in \mathbb{R}^{p \times q}$, provided $pq = mn$. We use vec to represent the vectorization operator and $\mathbf{1}^T \in \mathbb{R}^{n^2}$ to represent a vector of all ones. For details of the above derivation, see the Appendix. It can be shown that $\tilde{K} = K - \bar{K}$ is the descent direction for Φ_1 [13, See Lemma 4.1]. The Armijo-Goldstein line search method can then be used to determine a step size s to ensure $(K + s\tilde{K}) \in \mathbb{K}$, i.e., stability of (13) is maintained. The iterative process continues till we obtain $\nabla\Phi_1(K) \approx 0$.

¹We denote $N_d(c)$ simply as N_d throughout this subsection as c is constant for $\mathbf{P1}_{\text{in}}$.

4.1.2 F -min Step

The solution of the F -min step is well-known in the literature [12, Sec. 4.4.3] as:

$$F_{ij} = \begin{cases} (1 - \frac{a_{ij}}{|V_{ij}|})V_{ij}, & \text{if } |V_{ij}| > a_{ij}, \\ 0, & \text{otherwise,} \end{cases} \quad (37)$$

where $a_{ij} = \frac{\lambda}{\rho}W_{ij}$. Note that large values of λ will induce more sparsity, and therefore may lead to a sudden increase in J . Therefore, λ must be increased in small steps. The regularization path, for example, can be logarithmically spaced from $0.01\lambda_{max}$ to $0.95\lambda_{max}$, where λ_{max} is ideally the critical value of λ above which the solution of $\mathbf{P1}_{in}$ is $K = F = 0$ [12]. In our simulations, $\lambda_{max} = 1$.

4.2 Outer Loop

The outer-loop of our algorithm designs τ_o and c with bandwidth constraint (28) and updates the weight matrix W for minimizing the weighed l_1 norm in (32). Co-design of K in this loop is necessary to ensure stability as τ_o and c change. Let $K^* = F^*$ and Θ^* be the output of the last converged inner loop with $U^* = K^* - \frac{1}{\rho}\Theta^*$. Programs $\mathbf{P1}_{o1}$ and $\mathbf{P1}_{o2}$ directly design (K, τ_o) and (K, c) , respectively, in sequence as follows:

$$\mathbf{P1}_{o1} : \underset{K, \tau_o, P}{\text{minimize}} \hat{J}(K, \tau_o) + \frac{\rho}{2}\|K - U^*\|_{\mathbb{F}}^2, \quad (38a)$$

$$\text{subject to } \delta S(\tau_o) \leq 0, \quad (38b)$$

$$\text{SDP in Eq. (25),} \quad (38c)$$

$$\mathbf{P1}_{o2} : \underset{K, c, L}{\text{minimize}} \hat{J}(K, c) + \frac{\rho}{2}\|K - U^*\|_{\mathbb{F}}^2, \quad (38d)$$

$$\text{subject to } \delta S(c) \leq 0, \quad (38e)$$

$$\text{SDP in Eq. (27),} \quad (38f)$$

where $\hat{J}(K, \tau_o) = \text{Tr}(\mathcal{B}^T P \mathcal{B})$, $\hat{J}(K, c) = \text{Tr}(L C^*{}^T C^*)$, $C^* = (K^* \circ \mathcal{I}_d)N_d^T(c^*) + (K^* \circ \mathcal{I}_o)N_o^T$. We next present our main algorithm to show the iterative solutions of $\mathbf{P1}_{o1}$ and $\mathbf{P1}_{o2}$ beginning from a known stabilizing tuple (K^*, τ_o^*, c^*) .

4.3 Main Algorithm

Our main algorithm is listed in Algorithm 1; the following points explain its key steps.

- Using $\mathbf{P1}_{o1}$, we first co-design a stabilizing pair (\hat{K}, τ_o) from an initial tuple $(K^*, \tau_o^*, c^*) \in \mathcal{K}$. The two are designed together as the initial K^* may not be stabilizing for τ_o satisfying the bandwidth constraint (30).
- We then use the solution of $\mathbf{P1}_{o1}$, i.e., $(\hat{K}, \tau_o, c^*) \in \mathcal{K}$ as the initial point for $\mathbf{P1}_{o2}$ to find an updated pair (K, c) . From Proposition 1, $\delta S(c)$ in (30) is convex in c . Let c_{min} be the minimizer of $\delta S(c)$. If \hat{K} is stabilizing for c_{min} , then instead of co-designing (K, c) , we can directly set $c = c_{min}$ and $K = \hat{K}$, and then use a procedure similar to K -min to minimize $J(K)$ starting from \hat{K} .
- The inner-loop begins with $(K, \tau_o, c) \in \mathcal{K}$. K is updated in the direction of decreasing J and increasing sparsity while τ_o and c remain constant.
- Following [1, Sec. III-D] and [12, Sec. 3.4.1], ρ in (34) is chosen to be sufficiently large to ensure the convergence of the inner ADMM loop. Since J is nonconvex, convergence of this loop, in general, is not guaranteed, as is commonly seen in the sparsity promoting literature [1]. However, large values of ρ have been shown to facilitate convergence. We use $\rho = 100$ for our simulations. The stopping criterion for the inner loop in Line 8 of Algo. 1 follows [12, Sec. 3.3.1].

Algorithm 1: Main Algorithm

```
1 Input: Initial feasible point  $(K_o^*, \tau_o^*, c^*) \in \mathcal{K}$ 
2 for  $\lambda_i = 0.01\lambda_{max}$  to  $0.95\lambda_{max}$  do
3   Input:  $K^*$ ,  $\tau_o^*$  and  $c^*$  stabilizing for (5)
4   for 1 to Maximum Reweighted Steps do
5     Solve P1o1 using  $K^*$ ,  $\tau_o^*$ ,  $c^*$  to get  $\hat{K}$ ,  $\tau_o$ 
6     Solve P1o2 using  $\hat{K}$ ,  $\tau_o$ ,  $c^*$  to get updated  $K$ ,  $c$ .
7     Input: Inner loop initial:  $K$ ,  $c$ ,  $\tau_o$ 
8     while ADMM Stopping Criteria not met do
9        $K$ -min : Solve (34a) for  $K_{k+1}$ 
10       $F$ -min : Solve (34b) for  $F_{k+1}$ 
11      Update  $\Theta$  using (34c)
12    end
13    Result:  $K^* = K$ ,  $\tau_o^* = \tau_o$ ,  $c^* = c$ .
14    Update  $W$  using  $K^*$  from (32).
15    Update  $S^*$  using  $N_{row}(K^*)$ ,  $N_{col}(K^*)$ ,  $N_{off}(K^*)$ ,  $\tau_o^*$  and  $c^*$  from (28).
16  end
17 end
18 Result:  $K$ ,  $\tau_o$  and  $c$  are obtained for  $\lambda_i$ .
```

5 Simulations Results

5.1 Delay-Design With No Bandwidth Constraints

We first present simulations where only the outer loop is iterated without considering any bandwidth constraint in Algorithm 1. This example shows that the relative magnitudes of τ_d and τ_o for obtaining minimum \mathcal{H}_2 -norm can be significantly different for different systems. Absence of the bandwidth cost, as indicated before, will lead to the trivial solution $\tau_o = 0$, $\tau_d = 0$. To avoid this, we impose a simple artificial constraint $|(\tau_d - \tau_d^*) + (\tau_o - \tau_o^*)| \leq \epsilon$ where $0 < \epsilon \ll 1$ is a small tolerance, and $(K^*, \tau_o^*, \tau_d^*) \in \mathcal{K}$ is the initial point for every iteration. This initial tuple is replaced by the newly designed $(K, \tau_o, \tau_d) \in \mathcal{K}$ at the end of every iteration. We simulate two randomly generated models I_a and I_b with $A \in \mathbb{R}^{5 \times 5}$, $B = B_w = I_n$, $K^* = K_{LQR}$, $Q = R = I_n$ for two different initial conditions as part of Case A. The logarithm of ratios of J , $\tau_d + \tau_o$, τ_o and c with respect to their respective minima are plotted in Fig. 2.

Case A: Right and left axis of all the sub-figures in Fig. 2 show system I_a and I_b with (c^*, τ_o^*) chosen as (0.489, 0.141) and (0.833, 0.108), respectively. For both the systems, J in Fig. 2 (a) is seen to be decreasing as $\tau_o + \tau_d$ decreases. This is expected as \mathcal{H}_2 -performance improves with a decrease in the overall delay. Fig. 2 (a), (c) and (d) show that for achieving a lower J , the model I_a requires a lower τ_o and a higher c , while I_b requires a higher τ_o and a lower c . We can infer that obtaining a better \mathcal{H}_2 -performance can demand completely different relative magnitudes of τ_d and τ_o depending on the system model and the initial conditions. Thus, this example validates the motivation of our problem in determining the trade-off between τ_d and τ_o .

5.2 Delay-Design with Bandwidth Constraints

We next validate Algorithm 1. To illustrate its benefits, we compare it to an algorithm that consists of only the inner ADMM loop, referred to as the *constant-delay* algorithm. Both algorithms start

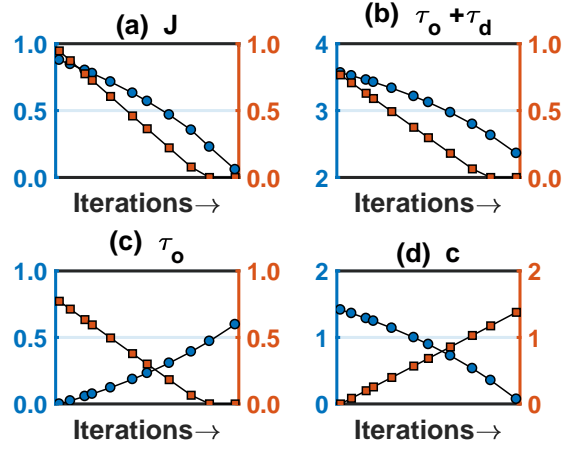


Figure 2: (a), (b), (c), (d) show normalized J , $\tau_o + \tau_d$, τ_o and c vs iterations - Right axis for Model I_a (■), Left axis for Model I_b (●).

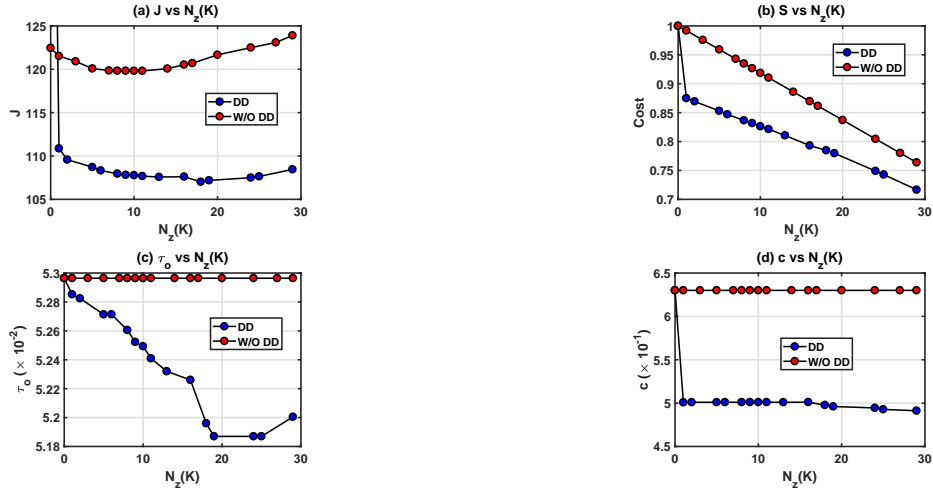


Figure 3: Case B-I (a), (b), (c), (d) show J , S , τ_o and c vs N_z where N_z is the number of zero elements of K . 'DD' and 'W/O DD' indicate Algorithm 1 and constant-delay algorithms respectively.

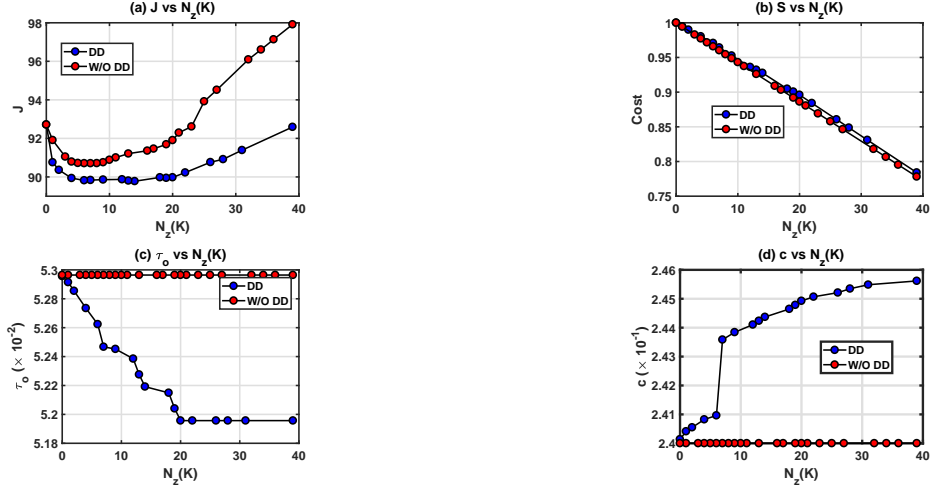


Figure 4: Case B-II (a), (b), (c), (d) show J , S , τ_o and c vs $N_z(K)$ where N_z is the number of zero elements of K . ‘DD’ and ‘W/O DD’ indicate Algorithm 1 and constant-delay algorithms respectively.

from $(K^*, \tau_o^*, \tau_d^*) \in \mathcal{K}$. The delays τ_o^* and τ_d^* are kept constant throughout the constant-delay algorithm. We present the simulations for two randomly generated LTI models in Case B-I and B-II with $A \in \mathbb{R}^{10 \times 10}$ and $B = B_w = Q = R = I_n$. We denote the number of zero elements of K by $N_z(K)$.

Case B-I: We consider $m_{cp} = 53$, $m_{cc} = 38$, $(c^*, \tau_o^*) = (0.63, 0.053)$ for this case. Fig. 3 (a), (b), (c) and (d) show J , normalized bandwidth cost S with respect to initial cost, τ_o and c , respectively. The initial delay ratio c^* is such that $c_{min} = 0.5007 < c^*$, and K^* is stabilizing for this value of c_{min} . As a result, Algorithm 1 directly moves to $c = c_{min}$ at $N_z(K) = 1$ [see Section 4.3]. Further sparsification of K is carried out by Algorithm 1 along with the simultaneous changes in τ_o and c , such that the bandwidth cost constraint (7) is satisfied, and J remains optimal. Fig. 3 (c), (d) show this trade-off between τ_o and c , resulting in a significantly lower S obtained for Algorithm 1 as compared to the constant-delay algorithm in Fig. 3 (b). The delay τ_o first decreases till $N_z(K) = 13$, while c remains nearly constant. As sparsity of K increases further, τ_o begins to increase, while c decreases. This indicates that the decrease in τ_o is prioritized by Algorithm 1 till $N_z(K) = 13$. The priority later shifts to decreasing c as sparsity increases. The shifting priority of one delay over another highlights the implicit relationship between K , τ_o and τ_d .

Case B-II: We consider another randomly generated $A \in \mathbb{R}^{10 \times 10}$ with $(c^*, \tau_o^*) = (0.24, 0.089)$, $m_{cp} = 21$ and $m_{cc} = 31$. The initial conditions result in $c_{min} = 0.448 > c^*$ from (29). However, (K^*, c_{min}) is an unstable tuple, and therefore, we rely on $\mathbf{P1}_{o2}$ to co-design (K, c) . Fig. 4 (c), (d) show that as sparsity increases, Algorithm 1 continuously increases c and decreases τ_o to maintain optimality of J . As shown in Proposition 1, a decrease in τ_o increases the bandwidth cost S . However, since c moves towards c_{min} , S in Fig. 4 (b) remains comparable to that of the constant-delay algorithm despite the continuous decrease in τ_o . Fig. 4 (a), (b) show that as a trade-off for slightly higher S from Algorithm 1, we obtain a lower J as compared to the constant-delay algorithm for all the sparsity levels.

6 Conclusion

This paper presented a co-design for network delays and sparse controllers to improve the \mathcal{H}_2 -performance of delayed LTI systems. The challenges of co-design arising from the implicit functional relationships between the delays, the sparse controller, and the \mathcal{H}_2 -norm are overcome by developing a hierarchical algorithm, whose inner loop and outer loop are based on ADMM and SDP relaxations, respectively. Numerical simulations show the effectiveness of the design, while bringing out interesting observations about these implicit relationships. Our future work will be to extend this design to uncertain LTI models using reinforcement learning.

Appendix: Proofs

Proof of Lemma 1: The ij -th block of \tilde{A} is given as:

$$\tilde{A}_{ij} = \begin{cases} \sum_{k=1, k \neq j}^N \frac{1}{\theta_j - \theta_k} I_n, & i = 1, \dots, N-1 \& i = j \\ \frac{1}{\theta_j - \theta_i} \prod_{m=1, m \neq j, i}^N \frac{\theta_i - \theta_m}{\theta_j - \theta_m} I_n, & i = 1, \dots, N-1 \& i \neq j, \\ A, & i = N, j = 1, \dots, N. \end{cases} \quad (39)$$

Substituting (9) above, the diagonal and off-diagonal block matrices of the first $N-1$ block rows are given by:

$$a_{ik} = - \left(\sin \left(\frac{(2N-i-k)\pi}{2(N-1)} \right) \sin \left(\frac{(k-i)\pi}{2(N-1)} \right) \right)^{-1}, \quad (40a)$$

$$\tilde{A}_{ii} = \frac{1}{\tau_o} \sum_{k=1, k \neq i}^N a_{ik} I_n, \quad \tilde{A}_{ji} = \frac{a_{ji}}{\tau_o} \prod_{m=1, m \neq j, i}^N \frac{a_{jm}}{a_{im}} I_n, \quad (40b)$$

where $i, j \in \{1, \dots, N\}$. Therefore, Λ can be written as:

$$\Lambda_{ij} = \begin{cases} \tilde{A}_{ij}, & i = 1, \dots, N-1, j = 1, \dots, N, \\ \mathbf{0}, & i = N, j = 1, \dots, N. \end{cases} \quad (41)$$

The proof follows from (39), (40) and (41). ■

Proof of Lemma 2: Let $\vartheta_k = \cos \left(\frac{(N-k-1)\pi}{N-1} \right)$ for $k = \{0, \dots, N-1\}$. From (10) and (11), N_d can be written as:

$$N_d = [l_1(-\tau_d), \dots, l_N(-\tau_d)]^T \otimes I_n. \quad (42)$$

Using (9), (10a) and $c = \tau_d/\tau_o$ we can write

$$l_j(-\tau_d) = \prod_{m=1, m \neq j}^N \frac{-c - 0.5(\vartheta_{m-1} - 1)}{0.5(\vartheta_{j-1} - \vartheta_{m-1})}. \quad (43)$$

Using (42) and (43), N_d can be subsequently rewritten in the form of (18) where the j -th row of Γ contains the coefficients of $l_j(-\tau_d)$. From (43), $l_j(-\tau_d)$ is a product of $N-1$ affine terms in c whose coefficients are only dependent on N , and hence, Γ is constant for constant N . ■

Proof of Lemma 3: The proof of uniqueness of solution of (14) utilizes Lemma 1 and 2, and is similar to Theorem 2.1 in [13]. The differentiability of P can be proven by utilizing the uniqueness of solution of (14) and follows a procedure similar to Lemma 3.1 in [13]. ■

Proof of Theorem 1: The partial derivative of $J(K)$ is

$$J'(K)dK = \text{Tr}(P'(K)\mathcal{B}\mathcal{B}^T) = \text{Tr}(\nabla J(K)^T dK), \quad (44)$$

where $dK \in \mathbb{R}^{m \times n}$. Post-multiplying (22) with L and taking its trace, we obtain the following equation using (44).

$$\text{Tr}(dK^T \nabla J(K)) = \text{Tr}((dK \circ \mathcal{I}_d)^T GLN_d + (dK \circ \mathcal{I}_o)^T GLN_o). \quad (45)$$

Using the property $\text{Tr}((X \circ Y)^T Z) = \text{Tr}(X^T(Y \circ Z))$ [14, Prob. 8.37], where $X, Y, Z \in \mathbb{R}^{m \times n}$ in (45), we get (24). Using (20), (21) in Lemma 3 and a similar procedure as above, we obtain

$$J'(\tau_o) = -\frac{1}{\tau_o^2} \text{Tr}(\Lambda^T PL + LPA), \quad (46)$$

$$J'(c) = \text{Tr}(N'_d K_d^T GL + LG^T K_d N'_d{}^T). \quad (47)$$

We can subsequently obtain (23) from (46) and (47). ■

Proof of Theorem 2: Using $\phi_0, \phi_1, \psi_0, A_1$ and $\tilde{\Delta}\tilde{C}$ as stated in the theorem, we define ϕ and ψ using Lemma 1 as:

$$\begin{aligned} \phi &= \phi_0 + \phi_1 + \phi_2, \quad \phi_2 = A_1^T \Delta P + \Delta P A_1^T, \\ \psi &= \psi_0 + \psi_1, \quad \psi_1 = \tilde{\Delta}\tilde{C}^T R \tilde{\Delta}\tilde{C}. \end{aligned} \quad (48)$$

The equation $\phi + \psi = 0$ is equivalent to (14) for (K, ω_o, c^*) with $\omega_o = 1/\tau_o$ and therefore, (K, ω_o, c^*) is a stabilizing tuple if $\phi + \psi \leq 0$ is satisfied. This inequality will be satisfied by ϕ and ψ if they satisfy $\lambda_{max}(\phi) + \lambda_{max}(\psi) \leq 0$ [15, Theorem 4.3.1 (Weyl)]. Therefore, the following inequality is a sufficient condition for stability:

$$\phi_0 + \phi_1 + \psi_0 + \lambda_{max}(\phi_2) + \lambda_{max}(\psi_1) \leq 0. \quad (49)$$

Equation (49) can be equivalently written as:

$$\phi_0 + \phi_1 + \psi_0 + \alpha I \leq 0, \quad \alpha \geq \lambda_{max}(\phi_2) + \lambda_{max}(\psi_1). \quad (50)$$

Following [15, Theorem 4.3.50] and [16, Theorem 1.2], $|\lambda_{max}(\phi_2)| \leq 2\|A_1^T \Delta P\|$, $|\lambda_{max}(\psi_1)| = \|\tilde{R}^{1/2} \tilde{\Delta}\tilde{C}\|^2$. Therefore, (25b)-(25c) yield the necessary α for satisfying (50). ■

Proof of Theorem 3: Let $\phi = \sum_{i=0}^4 \phi_i$ where $\phi_2 = A_1 \Delta L + \Delta L A_1^T$, $\phi_3 = A_2 L^* + L^* A_2^T$, $\phi_4 = A_2 \Delta L + \Delta L A_2^T$ and $A_2 = -\mathcal{B} \Delta K_d \Delta N_d^T$. The equation $\phi + \mathcal{B}\mathcal{B}^T = 0$ is equivalent to (15) for (K, τ_o^*, c) , and $\phi + \mathcal{B}\mathcal{B}^T \leq 0$ implies that (K, τ_o^*, c) is a stabilizing tuple. The rest of the proof can be obtained through similar arguments as Theorem 2.

Derivation of (36): Let $\bar{k} = \text{vec}(K)$. Using the property $\text{vec}(ABC) = (C^T \otimes A)B$, on (35), we obtain the following:

$$\begin{aligned} &(T_{dd}(\bar{k} \circ v_d) + T_{od}(\bar{v} \circ v_o)) \circ v_d + (T_{do}(\bar{k} \circ v_d) \\ &+ T_{oo}(\bar{k} \circ v_o)) \circ v_o + \rho(\bar{k} \circ v_d) + \rho(\bar{k} \circ v_o) = \mu. \end{aligned} \quad (51)$$

Since v_d and v_o are binary vectors, $(T_{dd}(\bar{k} \circ v_d)) \circ v_d = ((T_{dd} \circ \hat{V}_d^T)\bar{k}) \circ v_d$. Furthermore, $((T_{dd} \circ \hat{V}_d^T)\bar{k}) \circ v_d = (\hat{V}_d \circ T_{dd} \circ \hat{V}_d^T)\bar{k}$. Substituting this in (51),

$$\begin{aligned} & (\hat{V}_d \circ T_{dd} \circ \hat{V}_d^T + \hat{V}_d \circ T_{od} \circ \hat{V}_o^T \\ & + \hat{V}_o \circ T_{do} \circ \hat{V}_d^T + \hat{V}_o \circ T_{oo} \circ \hat{V}_o^T + \rho I_{n^2})\bar{k} = \mu. \end{aligned} \quad (52)$$

We get (36) from above, thereby completing the proof. ■

References

- [1] F. Lin, M. Fardad, and M. R. Jovanović, “Design of optimal sparse feedback gains via the alternating direction method of multipliers,” *IEEE Trans. Autom. Control*, vol. 58, no. 9, 2013.
- [2] M. Wytock and J. Z. Kolter, “A fast algorithm for sparse controller design,” *arXiv preprint arXiv:1312.4892*, 2013.
- [3] F. Lian, A. Chakraborty, and A. Duel-Hallen, “Game-theoretic multi-agent control and network cost allocation under communication constraints,” *IEEE J. Sel. Areas Commun.*, vol. 35, no. 2, 2017.
- [4] F. Lin and V. Adetola, “Sparse output feedback synthesis via proximal alternating linearization method,” *arXiv preprint arXiv:1706.08191*, 2017.
- [5] N. Negi and A. Chakraborty, “Sparse optimal control of LTI systems under sparsity-dependent delays,” in *2018 Annual American Control Conference (ACC)*. IEEE, 2018, pp. 2669–2674.
- [6] P. Naghshtabrizi, J. P. Hespanha, and A. R. Teel, “Stability of delay impulsive systems with application to networked control systems,” *TI Meas Control*, vol. 32, no. 5, pp. 511–528, 2010.
- [7] F. P. Kelly, A. K. Maulloo, and D. K. Tan, “Rate control for communication networks: shadow prices, proportional fairness and stability,” *Journal of the Operational Research society*, vol. 49, no. 3, pp. 237–252, 1998.
- [8] J. Barrera and A. Garcia, “Dynamic incentives for congestion control.” *IEEE Trans. Automat. Contr.*, vol. 60, no. 2, pp. 299–310, 2015.
- [9] K. Gu, J. Chen, and V. L. Kharitonov, *Stability of time-delay systems*. Springer Science & Business Media, 2003.
- [10] J. Vanbiervliet, W. Michiels, and E. Jarlebring, “Using spectral discretisation for the optimal h2 design of time-delay systems,” *International Journal of Control*, vol. 84, no. 2, pp. 228–241, 2011.
- [11] E. J. Candes, M. B. Wakin, and S. P. Boyd, “Enhancing sparsity by reweighted ℓ_1 minimization,” *Journal of Fourier analysis and applications*, vol. 14, no. 5, pp. 877–905, 2008.
- [12] S. Boyd, N. Parikh, E. Chu, B. Peleato, and J. Eckstein, “Distributed optimization and statistical learning via the alternating direction method of multipliers,” *Found. Trends Mach.*, vol. 3, no. 1, 2011.

- [13] T. Rautert and E. W. Sachs, “Computational design of optimal output feedback controllers,” *SIAM J Optim*, vol. 7, no. 3, 1997.
- [14] J. R. Schott, *Matrix analysis for statistics*. John Wiley & Sons, 2016.
- [15] R. A. Horn and C. R. Johnson, *Matrix analysis*. Cambridge university press, 2013.
- [16] M. Goldberg and E. Tadmor, “On the numerical radius and its applications,” *Linear Algebra Appl.*, vol. 42, pp. 263–284, 1982.